# Mechanical Properties of Cu-Cr system alloys with and without Zr and Ag

# Mechanical properties of Cu-Cr system alloys with and without Zr and Ag

Chihiro Watanabe*, Ryoichi Monzen, Kazue Tazaki

C. Watanabe *Corresponding author

Division of Innovative Technology and Science,

Kanazawa University, Kakuma-machi, Kanazawa 920-1192, Japan

e-mail: chihiro@t.kanazawa-u.ac.jp

R. Monzen

Division of Innovative Technology and Science,

Kanazawa University, Kakuma-machi, Kanazawa 920-1192, Japan

K. Tazaki

Division of Environmental Science and Engineering,

Kanazawa University, Kakuma-machi, Kanazawa 920-1192, Japan

**Abstract** The effects of addition of Zr and Ag on the mechanical properties of a Cu-0.5wt%Cr alloy have been investigated. The addition of 0.15wt%Zr enhances the strength and resistance to stress relaxation of the Cu-Cr alloy. The increase in strength is caused by both the decrease in inter-precipitate spacing of Cr precipitates and the precipitation of $Cu_5Zr$ phase. The stress relaxation resistance is improved by the preferentially forming $Cu_5Zr$ precipitates on dislocations, in addition to Cr precipitates on dislocations. The addition of 0.1wt%Ag to the Cu-Cr and Cu-Cr-Zr alloys improves the strength, stress relaxation resistance and bend formability of these alloys. The increase in strength and stress relaxation resistance is ascribed to the decrease in inter-precipitate spacing of Cr precipitates and the suppression of recovery during aging, and to the Ag-atom-drag effect on dislocation motion. The better bend formability of the Ag-added alloys is explained in terms of the larger post-uniform elongation of the alloys.

**Keywords** Cu-Cr-Zr system alloys, age hardening, Ag addition, mechanical properties, stress relaxation, bend formability

## Introduction

Conventionally, age-hardenable Cu-Cr-Zr system alloys are widely used in such applications as small electronic terminals and connectors. These applications require high strength and electrical conductivity as well as good bend formability. When such terminals and connectors are employed in an automobile engine room, they are exposed to an environment of relatively high temperature, and thus high resistance to stress relaxation is required for the long-term reliability of electrical terminals and connectors.

Although several studies have been performed on the mechanical and electrical properties of Cu-Cr-Zr system alloys [1-4], there are only a few investigations of the stress relaxation property and bend formability of these alloys [5]. Recently, a Cu-0.5wt%Cr-0.1wt%Ag system alloy called C18080 has been developed [6]. The Cu alloy containing Ag has better bend formability and stress relaxation behavior than conventional Cu-Cr system alloys. However, the causes for these improved properties have not yet been clarified. The purpose of this study is to metallographically examine the effects of addition of Zr and Ag on the strength, stress relaxation and bend formability of a Cu-0.5wt%Cr alloy.

## Experimental Procedure

Cu-0.5wt%Cr, Cu-0.5wt%Cr-0.03wt%Zr, Cu-0.5wt%Cr-0.1wt%Ag, Cu-0.5wt%Cr-0.15wt%Zr and Cu-0.5wt%Cr-0.15wt%Zr-0.1wt%Ag alloys were prepared by melting in an Argon atmosphere. The cast alloys were homogenized at 1000$^{o}$C for 24h in a vacuum and then cold-rolled to a 30% reduction in thickness. The rolled strips were solutionized at 1000$^{o}$C for 2h in an Argon atmosphere and then water quenched. Each strip was placed in a silica tube connected to a vacuum pump. The silica tube was partially evacuated to a vacuum of $10^{-3}$ Torr and back-filled with argon gas. This process was repeated to remove air from the tube. The solutionized alloys were cold-rolled to 80% reduction in thickness and then aged at 500$^{o}$C for various periods in the Argon atmosphere.

Microhardness tests were carried out using the Vickers method. The indentation was

made on the well-polished surface of the specimen pieces with a diamond square-based pyramid under a load of 0.3kg for a period of 20s. Tensile tests were performed using a static Instron type testing machine with a constant strain rate of $10^{-3}s^{-1}$ at room temperature. Electrical resistivity measurements were made using a standard four-point potentiometric technique at 20°C. The measurements were repeated 10 times to obtain one data point, reversing the current direction to eliminate the stray electromotive force. Transmission electron microscopy (TEM) was performed using a JEOL 2010FEF and a Hitachi H-9000NAR microscope at operating voltages of 200kV and 300kV. Thin foils for TEM observations were prepared using a twin-jet polishing method with a solution of 67% methanol and 33% nitric acid at -20°C and 5V.

180° bend tests [7] were carried out under various bend ratios of the bend radius *r* to the thickness *t* of specimen pieces. The bend tests were repeated five times for each alloy and bend ratio. The specimen pieces for the bend tests had a dimension of $30^{l} \times 10^{w} \times 0.25^{t}$ $mm^3$ and the bend axis was perpendicular to the direction of rolling. After the bend tests, the outer surface of the specimens was observed using an optical microscope. Bend formability of the alloys was judged from the minimum bend ratio, in which none of the five specimens exhibited cracks. According to the literature [8], cantilever stress relaxation tests were performed at 200°C in a Nitrogen atmosphere.

## Results

### Microstructure

The grain size of the present alloys solutionized at 1000°C was coarse, about 250μm. The TEM observations revealed that no precipitates existed in the solution-treated alloys. The aging of the alloys at 500°C for various periods after cold rolling to 80% reduction produced spherical precipitates in the Cu matrix. Fig. 1 is an example of the precipitates in a Cu-0.5%Cr specimen aged at 500°C for 1000s. Analyses of selected area diffraction patterns (SADPs) of several regions containing the precipitates revealed that the spherical precipitates

were a bcc Cr phase with the Nishiyama-Wassermann orientation relationship to the Cu matrix, which is in agreement with the relationship previously reported in the literature [9]. In a Cu-0.5%Cr-0.1%Ag specimen aged at 500$^{o}$C for 1000s no other precipitates existed, while in a Cu-0.5%Cr-0.15%Zr and a Cu-0.5%Cr-0.15%Zr-0.1%Ag specimen, disk-shaped precipitates were observed, as shown in Fig. 2, in addition to the Cr precipitates. There existed an extremely small number of disk-shaped precipitates in a Cu-0.5%Cr-0.03%Zr alloy, indicating that about 0.03%Zr atoms dissolve in the Cu matrix after aging at 500$^{o}$C for 1000s. Figs. 2 (a) and (b) depict the disk-shaped precipitates in a Cu-0.5%Cr-0.15%Zr specimen aged at 500$^{o}$C for 1000s, taken using the matrix [011] and [11$\bar{1}$] zone axes. From analyses of the SADPs, the disk-shaped precipitates were identified as a $Cu_5Zr$ phase with a $C15_b$ structure [10, 11]. In Fig. 2(b), the existence of a facet habit plane is clear. The orientation of the habit plane for the disk-shaped precipitates was determined by tilting the precipitates until the facet habit plane was accurately edge-on. The habit plane was parallel to the {111} plane.

Microhardness and electrical resistivity

Fig. 3 shows the hardness change of the present alloys during aging at 500$^{o}$C. The addition of Zr and Ag to the Cu-Cr alloys does not significantly change the microhardness after the solution treatment at 1000$^{o}$C and subsequent cold rolling. For each alloy, the peak hardness effect occurs after aging for about 1000s, and the hardness continues to decrease with further aging. The addition of Ag increases the hardness throughout the aging process. The Zr addition also enhances the hardness, and the effect is more pronounced for the alloy with 0.15%Zr. The alloy with Zr and Ag shows the highest hardness.

Fig. 4 presents the change in the electrical resistivity of the Cu-base alloys during aging at 500$^{o}$C. From the experimental data on the dependence of electrical resistivity on Cr, Ag or Zr concentration [12], it was judged that all atoms of 0.1%Ag, 0.03%Zr and 0.15%Zr were dissolved in the Cu matrix by the solution treatment at 1000$^{o}$C. As would be expected from the data on the Ag concentration dependence of resistivity [12], the addition of 0.1% Ag to the Cu-Cr or Cu-Cr-Zr alloy does not significantly affect the resistivity after the solution

treatment. The resistivity of each alloy exhibits first a gradual decrease, then a rapid decrease and finally an almost saturated value. The 0.1%Ag-added or 0.03%Zr-added alloy showed almost the same resistivity throughout the aging process as the Cu-Cr alloy, after the resistivity increment caused by 0.1%Ag or 0.03%Zr were factored in. In the early stage of aging, the alloy with 0.15%Zr has higher resistivity values than the alloy with 0.03%Zr, but after prolonged aging both alloys exhibit almost the same values. This result is attributed to the precipitation of the $Cu_5Zr$ phase during aging. The resistivity value at each time for the Cu-0.5%Cr-0.15%Zr-0.1%Ag alloy is nearly identical to that for the Cu-0.5%Cr-0.15%Zr alloy.

Table 1 summarizes the tensile properties and electrical resistivity of the present alloys aged at 500$^{o}$C for 1000s. The addition of Ag and/or Zr increases the 0.2% proof stress and tensile strength. On the other hand, the elongation is slightly reduced as the strength increases.

Bend formability

During bending deformation, a number of micro necks were first observed in the outer surface of specimen. Then, part of them grew, resulting in surface grooves. Figs. 5 (a) and (b) show the outer surface appearances after 180$^{o}$ bend tests of the Cu-Cr and Cu-Cr-Ag alloys aged at 500$^{o}$C for 1000s. A large number of grooves parallel to the bend axis are noticeable on both alloy sheets, but the features of the grooves are significantly different. In the Cu-Cr alloy, some of the grooves are deeply marked, and actual cracking is observed (Fig. 5(a)), while the Cu-Cr-Ag alloy exhibits relatively fine and uniformly scattered grooves (Fig. 5(b)) and no cracks. The improvement of bend formability with Ag is obvious. The bend formability of present alloys is listed in Table 1. The minimum bend ratios of the Cu-Cr and Cu-Cr-0.15Zr alloys are reduced by the addition of Ag. However, the Zr addition does not significantly affect the bend formability.

Stress relaxation property

Fig. 6 shows the stress relaxation rate against time for the present alloys tested at 200°C. The stress relaxation rate is defined as the ratio of the deflection upon unloading to the deflection upon loading on a cantilever [8]. The addition of Ag to the Cu-Cr alloy enhances the stress relaxation resistance. The addition of 0.03%Zr does not significantly change the rate, but the increase of the Zr content to 0.15% greatly improves the stress relaxation property. As a result, the Cu-Cr-Zr-Ag alloy shows the highest stress relaxation resistance.

## Discussion

### Effect of Ag and Zr on strength

It has been reported that the yield stress of Cu-Cr alloys containing Cr precipitates at room temperature is controlled by the Orowan mechanism at peak-age and over-age conditions [13, 14]. The Orowan stress is inversely proportional to the inter-precipitate spacing *l*. The increase in strength due to the addition of Zr and Ag can then be discussed by estimating *l*, which is taken as the square lattice spacing in parallel planes and is written as [15]

$$l = r\left[\left(\frac{2\pi}{3f}\right)^{1/2} - 1.63\right]. \qquad (1)$$

Here *r* is the average radius of precipitates and *f* is the volume fraction of precipitates. The average radius *r* of Cr precipitates was measured from bright-fields TEM images. To obtain statistically reliable data, more than 200 precipitates were analyzed for each alloy. The volume fraction *f* for the Cu-Cr alloy was determined by applying the values of electrical resistivity, before and after aging at 500°C for 1000s, to the experimental data regarding the dependence of electrical resistivity on Cr concentration [12]. For the Cu-Cr alloy with 0.1%Ag or 0.03%Zr, all of the trace atoms were assumed to be dissolved in the matrix. Then *f* was calculated after the resistivity increment caused by 0.1%Ag or 0.03%Zr addition was removed. In the case of the alloys with 0.15%Zr, *f* was estimated by assuming that 0.03%Zr

atoms were fully dissolved in the matrix after aging 500°C for 1000s. Table 2 lists the values of $r$ and $f$ for the present alloys. The number density $N$ of Cr precipitates was obtained from $r$ and $f$ using the equation of $N=3f / (4\pi r^3)$. The estimated values of $N$ and $l$ also are listed in Table 2, together with the values of $\sigma_{0.2}$. The values of $N$ for the 0.1%Ag-added and 0.03%Zr-added alloys are larger than that for the Cu-Cr alloy, indicating that both the Zr and Ag solutes promote the formation rate of Cr precipitates. Moreover, it is stated that the increase in $N$ or decrease in $l$ by adding 0.1%Ag and 0.03%Zr results in an increase in $\sigma_{0.2}$ due to the Orowan looping mechanism. It should be noted, however, that the value of $l$ for the 0.03%Zr-added alloy is smaller than that for the 0.1%Ag-added alloy, whereas the strength of the alloys is reversed.

Table 2 shows that the increase in the amount of Zr from 0.03% to 0.15% causes no change in $l$. As mentioned in above, in the Cu-Cr alloy with 0.15%Zr, the $Cu_5Zr$ phase precipitates in addition to the Cr precipitates. Thus, the increase in strength by the 0.15%Zr addition to the Cu-Cr alloy is attributable to the formation of $Cu_5Zr$ precipitates as well as the reduction in $l$. On the other hand, the addition of 0.1%Ag to the Cu-Cr-Zr alloy did not significantly change the average size and spacing of not only the Cr precipitates but also the $Cu_5Zr$ precipitates, but did increase the strength. Therefore, it is necessary to discuss another factor responsible for the increase in strength by the Ag addition.

Figs. 7 (a) and (b) present the stress-strain curves of the Cu-Cr and Cu-Cr-Ag alloys, and the Cu-Cr-0.15%Zr and Cu-Cr-0.15%Zr-Ag alloys, aged at 500°C for 1000s after 80% cold-rolling. It can be seen that the work-hardening rates of the alloys without Ag are larger than those of the alloys with Ag. It is well known that the work-hardening rate in the initial stage of deformation caused by Orowan loops around non-shearable particles depends strongly on the volume fraction of the particles [16, 17]. Since the volume fractions of the Cr precipitates are nearly identical for the alloys with and without Ag, as shown in Table 2, a difference in dislocation density between the alloys with and without Ag can be pointed out as the origin of the discrepancy in work-hardening rate. As previously reported by Gallagher *et al*. [18], the addition of Ag to Cu causes a reduction in stacking-fault energy. The annihilation of dislocations should certainly occur during aging at 500°C after cold rolling, since partial

recrystallization was observed in over-aged Cu-Cr, Cu-Cr-0.03%Zr and Cu-Cr-Ag specimens. Therefore, it is most likely that the suppression of recovery during aging by the Ag addition to the Cu-Cr and Cu-Cr-Zr alloys contributes greatly to the increase in strength and the decrease in the work- hardening rate. Therefore, the increase in strength due to the addition of Ag can be attributed to the decrease in inter-precipitate spacing of Cr precipitates and the suppression of recovery during aging.

Effect of Ag on bend formability

It is commonly known that the bend formability of materials is related to their strength and ductility, and increasing strength or decreasing ductility is often accompanied by worse bend formability [19, 20]. As can be seen in Table 1, the addition of Ag not only increases the strength and decreases the elongation, but also improves the bend formability. Thus, the effect of Ag addition on bend formability cannot be explained by the change in strength or ductility. Hatakeyama *et al.* have reported that the bend formability of tempered Cu alloys depends on the amount of non-uniform deformation and that an increase in the post-uniform elongation leads to better bend formability [21]. Therefore, we investigated the relationship between the post-uniform elongation and bend formability of the present alloys. The results are shown in Table 3. The addition of Ag increases the post-uniform deformation. Thus, the improvement of bend formability by the Ag addition can be understood to arise owing to the increase in post-uniform elongation.

Effect of Ag and Zr on resistance to stress relaxation

Since stress relaxation tests were performed at a relatively low temperature of 200$^{o}$C in the present study, the stress relaxation is likely to occur by logarithmic creep caused by the relatively-short range motion of dislocations [19, 22]. Thus, the stress relaxation depends on the mobility and density of mobile dislocations.

It is well known that the mobility of dislocations decreases when they are dragging

their atmospheres of solute atoms behind them. If the improvement of the stress relaxation property of alloys by the Ag addition in Fig. 6 is attributable to the drag of atmosphere of Ag atoms, the occurrence of serrations in tensile stress-strain curves of the alloys with Ag may be expected. However, no serrations were observed. Instead, tensile tests of a Cu-2.0wt% Ag alloy were carried out at 20 and 200$^{o}$C to reveal the effect of solute Ag atoms on the stress relaxation property. Serrations did not occur in the stress-strain curve at 20$^{o}$C but were formed at 200$^{o}$C, as shown in Fig. 8. This phenomenon is caused by the Portevin-Le Chatelier effect which shows such a type of temperature dependence. Therefore, the improvement of the stress relaxation property by the Ag addition can be ascribed to the viscous glide motion of dislocations dragging the Ag solute.

Since the addition of 0.03%Zr to the Cu-0.5%Cr alloy did not change the stress relaxation property of the alloy, as seen in Fig. 6, the development of the stress relaxation property due to the addition of 0.15%Zr is brought about by precipitation of $Cu_5Zr$ particles. TEM observations of a Cu-Cr-0.15%Zr alloy aged at 500$^{o}$C for 2h after 20% cold-rolling revealed that Cr and $Cu_5Zr$ precipitates formed preferentially on dislocations, as exemplified in Figs. 9 (a) and (b). The number density of mobile dislocations in the Cu-Cr-0.15%Zr alloy should accordingly be lower than that in the Cu-Cr-0.03%Zr alloy, because of the pinning of dislocations by the Cr and $Cu_5Zr$ precipitates. This explains the higher resistance to stress relaxation for the alloy with 0.15%Zr.

## Conclusions

Investigations of the mechanical property of Cu-0.5wt%Cr alloys with and without Ag and Zr by means of microstructural observations have yielded the following conclusions:

(1) Adding 0.15wt%Zr to the Cu-0.5wt%Cr alloy brings about the improvement in strength and stress relaxation property. The Zr addition decreases the inter-precipitate spacing of Cr precipitates and forms disk-shaped $Cu_5Zr$ precipitates, resulting in the increase in strength. The higher resistance to stress relaxation of the Zr-added alloy is attributed to the lower density of mobile dislocations due to the preferential formation of $Cu_5Zr$

precipitates on dislocations.

(2) The strength, bend formability and stress relaxation property are enhanced by 0.1wt%Ag added to the Cu-0.5wt%Cr and Cu-0.5wt%Cr-0.15wt%Zr alloys. The increase in strength by the Ag addition is ascribed to the decrease in inter-precipitate spacing of Cr precipitates and to the suppression of recovery during aging. The improvement of bend formability and stress relaxation property can be explained by the increase in post-uniform elongation and by the viscous glide motion of dislocations dragging Ag atoms.

**Acknowledgements** This work has been supported by a Grant-in-Aid for Scientific Research (C) from the Japan Society for Promotion of Science (JSPS) under Grant No. 17560614. We also thank Mr. K. Higashimine of the Center for Nano Materials and Technology, Japan Advanced Institution Science and Technology, for the TEM observations.

## References


1. Tang NY, Taplin DMR, G. L. Dunlop (1985) Mater Sci Technol 1:270
2. Correia JB, Davies HA, Sellars CM (1997) Acta Mater 45:177
3. Batra IS, Dey GK, Kulkarni UD, Banerjee S (2001) J Nucl Mater 299:91
4. Batra IS, Dey GK, Kulkarni UD, Banerjee S (2003) Mater Sci Eng A356:32
5. Ishida M, Iwamura T, Suzuki T, Deliand F, (2003) J JRICu 42:153
6. Seeger J, Kuhn A, Bogel A, Buresch I (2002) Metall 56:289
7 Standard Test Method for Bend Test for Determining the Formability of Copper and Copper Alloy Strip in “ASTM Test Method” (ASTM international, West Conshohocken, 2004) p. 758.
8. Standard Test Methods for Stress Relaxation for Materials and Structures in “ASTM Test Method” (ASTM international, West Conshohocken, 2004) p. 397
9. Fujii T, Nakazawa H, Kato M, Dahmen U, (2000) Acta Mater 48:1033
10. Forey P, Glimois JL, Foren JL, Devely G, Devely G (1980) C R Acad Sc Paris 291:177
11. Kneller E, Khan Y, Gorres U (1986) Z Metallkd **77**:43
12. Komatsu S (2002) J JCBRA 41:1
13. Long NJ, Loretto MH, Lloyd CH (1980) Acta Metall 28:709
14. Holzwarth U, Stamm H (2000) J Nucl Mater 279:31
15. Martin JW in “Micromechanism in Particle-Hardened Alloys” (Cambridge Univ. Press, Cambridge, 1980) p. 44.
16. Tanaka K, Mori T (1970) Acta Metall 18:931
17. Brown LM, Clarke DR (1975) Acta Metall **23**:821
18. Gallagher PCJ (1970) Metall Trans 1:2429
19. Miyake J (1997) J JCBRA 38: 1
20. Usami T, Hirai T, Kurihara M, Oyama Y, Eguchi T (2001) J JCBRA 40:294
21. Hatakeyama K, Sugawara A, Tojyo T, Ikeda K (2002) Mater Trans 43: 2908
22. Sato E, Yamada T, Tanaka H, Jinbo I (2005) J Jpn Inst Light Metals 55:604

**Figure and Table captions**

Fig. 1 TEM image of Cr precipitates in a Cu-0.5%Cr alloy aged at 500°C for 1000s.

Fig. 2 TEM images of $Cu_5Zr$ precipitates in a Cu-0.5%Cr-0.15%Zr alloy aged at 500°C for 1000s. The zone axes are parallel to (a) [011] and (b) $[11\bar{1}]$.

Fig. 3 Age-hardening curves of Cu-Cr system alloys aged at 500°C.

Fig. 4 Change in the electrical resistivity of Cu-Cr system alloys during aging at 500°C.

Fig. 5 Optical micrographs showing the surface appearances after 180° bend tests (with a bend ratio $r$ / $t$ of 1) of (a) Cu-0.5%Cr and (b) Cu-0.5%Cr-0.1%Ag alloys aged at 500°C for 1000s.

Fig. 6 Stress relaxation property for Cu-Cr system alloys aged at 500°C for 1000s, tested at 200°C.

Fig. 7 Stress-strain curves of (a) Cu-0.5%Cr and (b) Cu-0.5%Cr-0.15%Zr alloys with and without 0.1%Ag, aged at 500°C for 1000s.

Fig. 8 Stress-strain curves for a Cu-2wt%Ag alloy tested at 20 and 200°C.

Fig. 9 TEM images of (a) Cr and (b) $Cu_5Zr$ precipitates on dislocations in a Cu-0.5%Cr-0.15%Zr alloy aged at 500°C for 2h after 20% cold rolling.

Table 1 Tensile properties, electrical conductivity and bend formability for Cu-0.5%Cr, Cu-0.5%Cr-0.1%Ag, Cu-0.5%Cr-0.03%Zr, Cu-0.5%Cr-0.15%Zr and Cu-0.5%Cr-0.15%Zr-0.1%Ag alloys, aged at 500°C for 1000s.

Table 2 0.2% proof stress $\sigma_{0.2}$, average radius $r$ of Cr precipitates, volume fraction $f$, inter-precipitate spacing $l$ and number density $N$ for Cu-0.5%Cr, Cu-0.5%Cr-0.1%Ag, Cu-0.5%Cr-0.03%Zr, Cu-0.5%Cr-0.15%Zr and Cu-0.5%Cr-0.15%Zr-0.1%Ag alloys, aged at 500$^{o}$C for 1000s.

Table 3 Elongation, post-uniform elongation, elongation / post-uniform elongation and bend formability for Cu-0.5%Cr, Cu-0.5%Cr-0.1%Ag, Cu-0.5%Cr-0.03%Zr, Cu-0.5%Cr-0.15%Zr and Cu-0.5%Cr-0.15%Zr- 0.1%Ag alloys, aged at 500$^{o}$C for 1000s.

**Figure 1**

Click here to download high resolution image

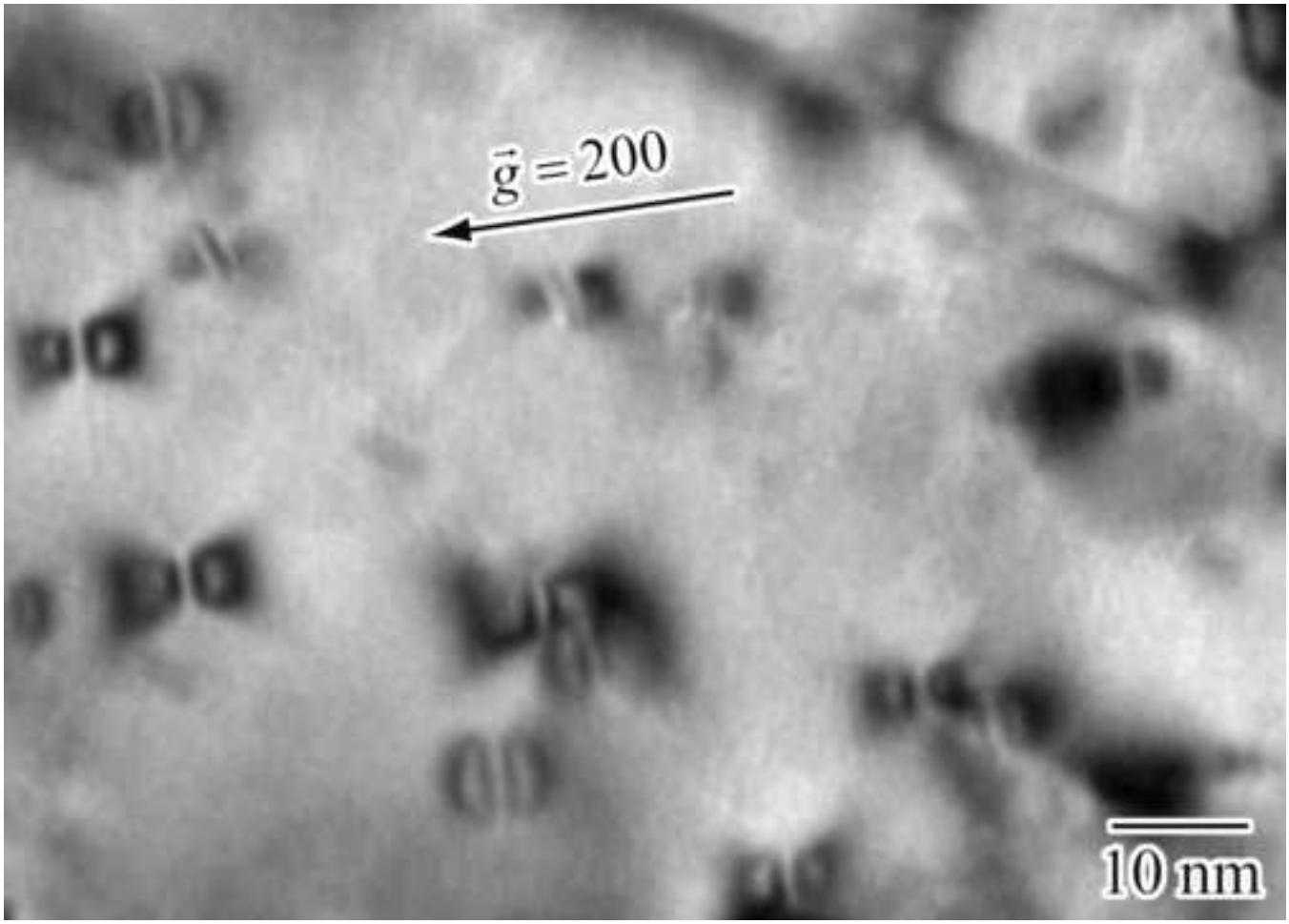

**Figure 2(a)**

**Click here to download high resolution image**

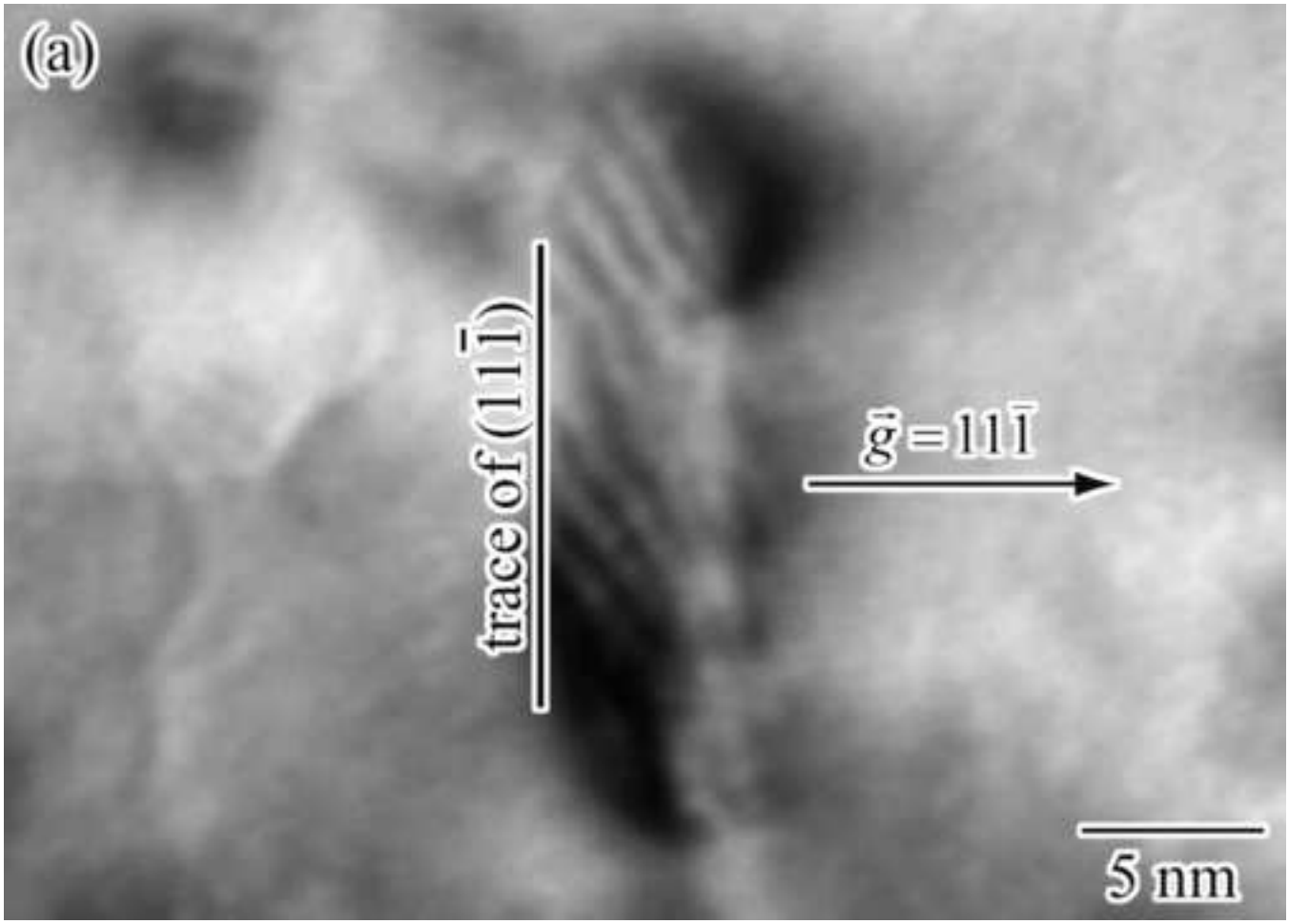

**Figure 2(b)**

**Click here to download high resolution image**

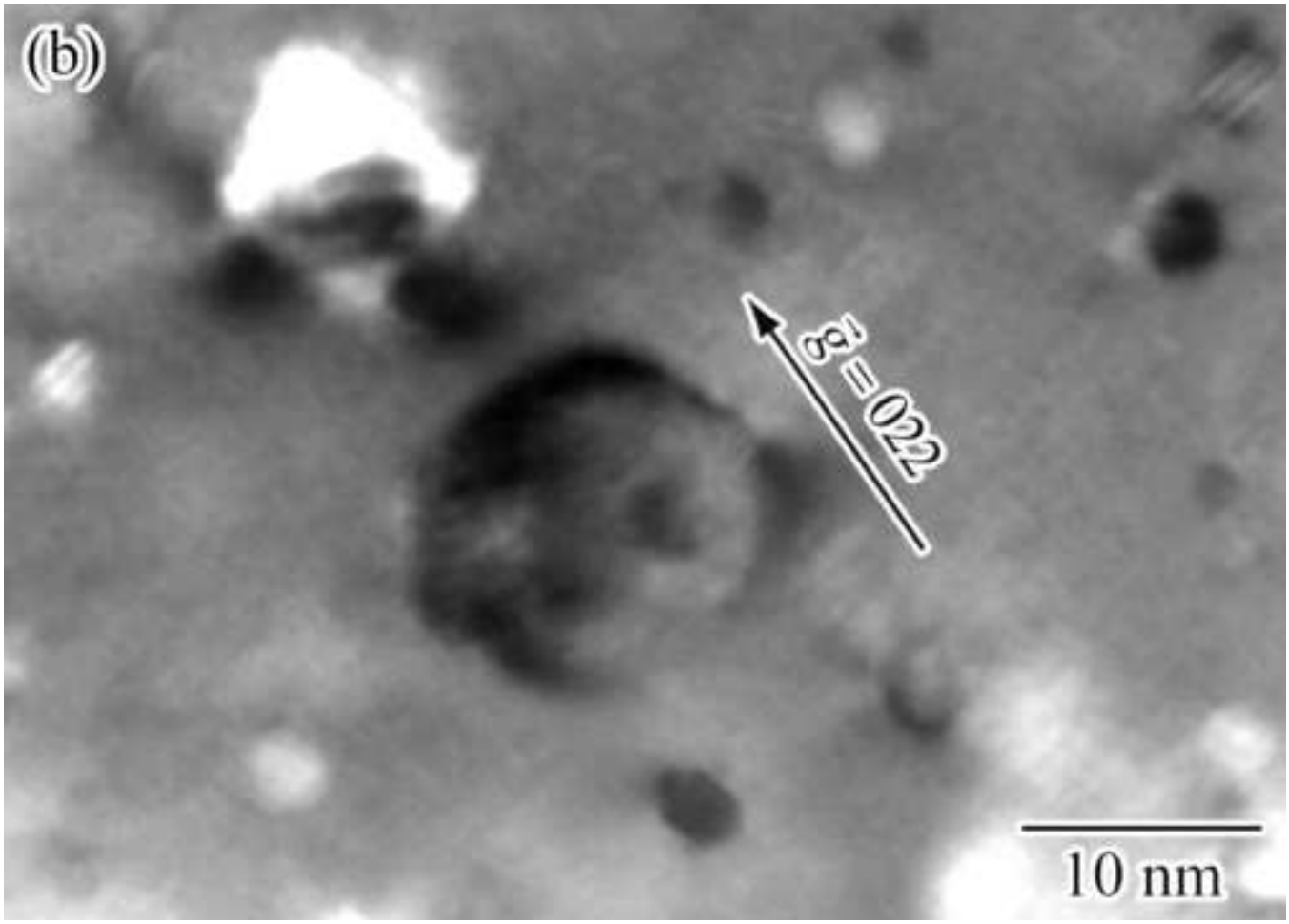

**Figure 6**

Click here to download Figure: Fig06.eps

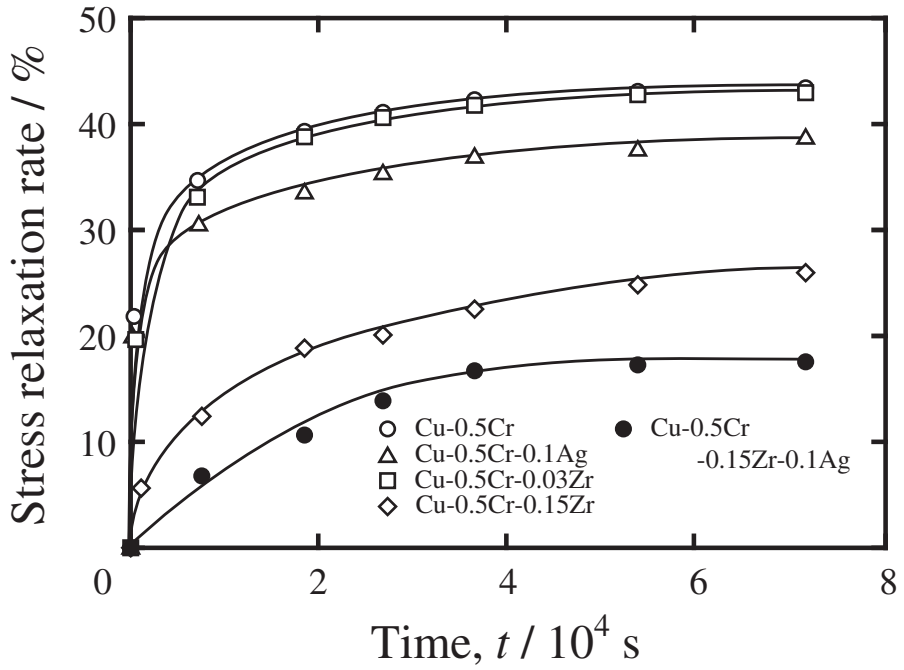

**Figure 7(b)**

Click here to download Figure: Fig07(b).eps

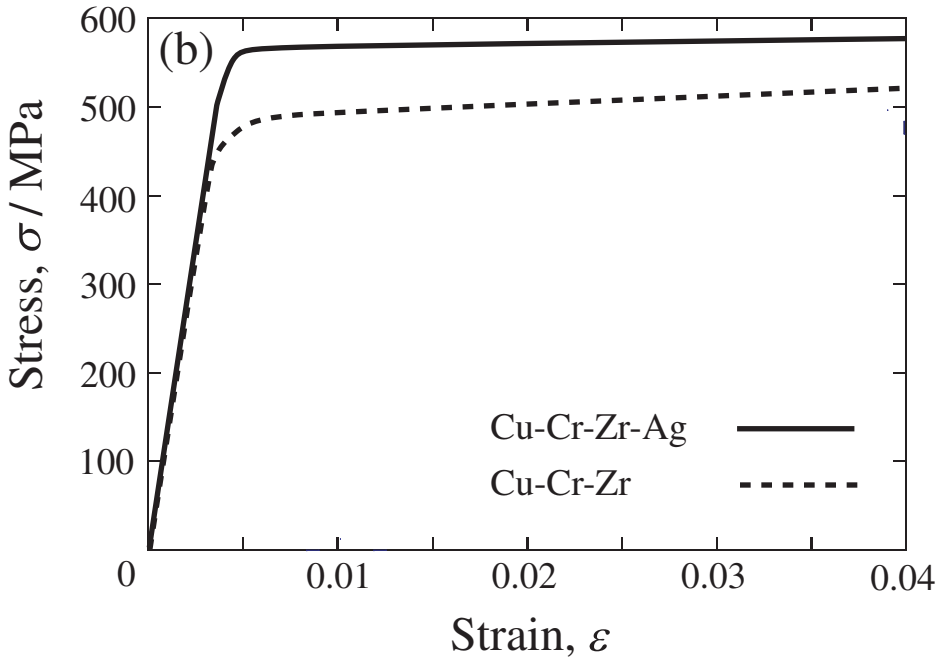

**Figure 8**

Click here to download Figure: Fig08.eps

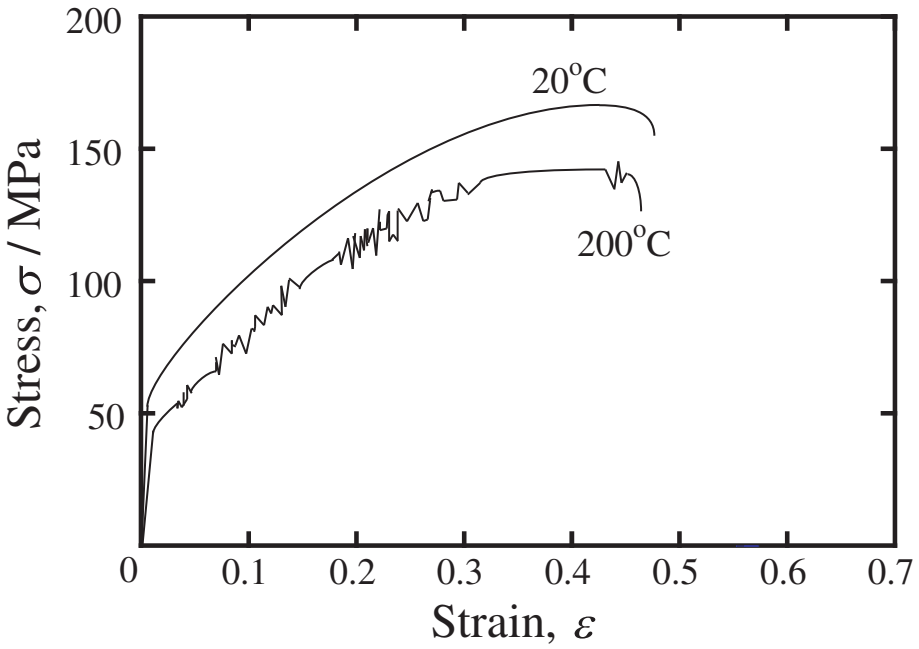

**Figure 9(a)**
**Click here to download high resolution image**

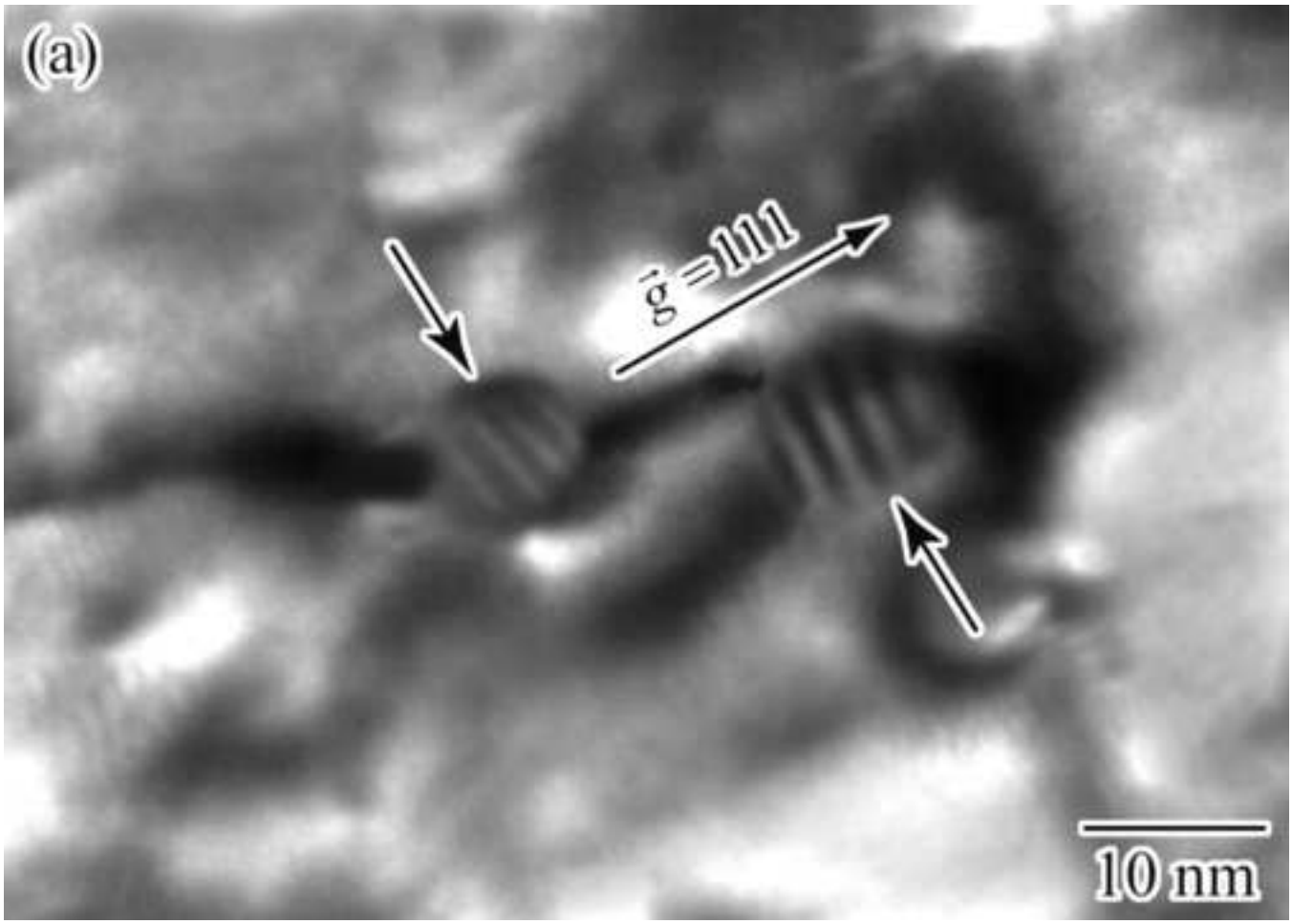

**Figure 9(b)**

**Click here to download high resolution image**

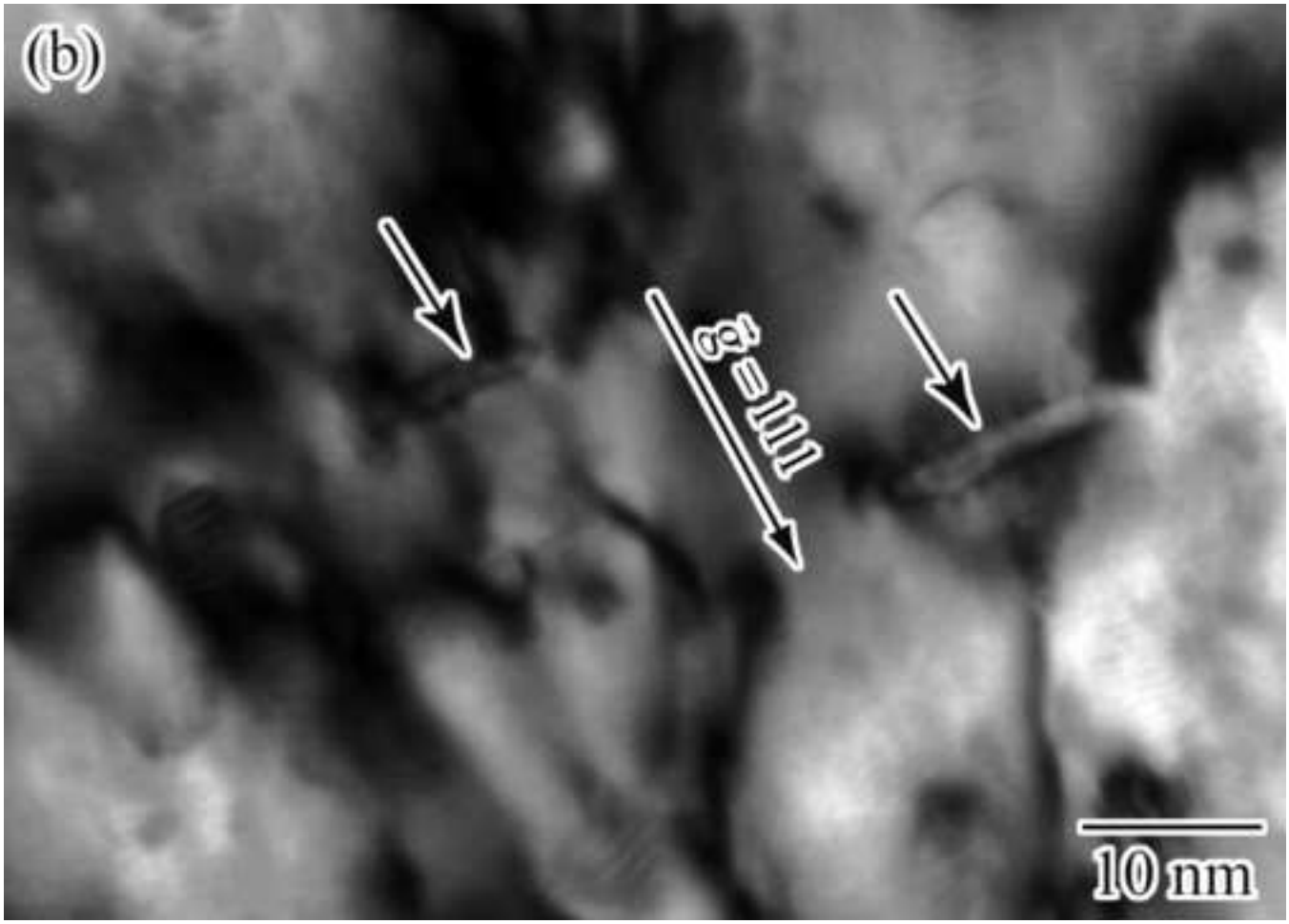

**Table 3**

Click here to download Table: Table3.eps

| Alloy composition (wt%) | Elongation (%) | Post-uniform elongation (%) | Elongation / Post-uniform elongation | Bend formability ( $r$ / $t$ ) |
|---|---|---|---|---|
| Cu-0.5Cr | 13 | 3.5 | 3.7 | 2 |
| Cu-0.5Cr-0.1Ag | 12 | 4.8 | 2.5 | 1 |
| Cu-0.5Cr-0.03Zr | 12 | 3.5 | 3.4 | 2 |
| Cu-0.5Cr-0.15Zr | 11 | 3.5 | 3.4 | 2 |
| Cu-0.5Cr-0.15Zr-0.1Ag | 11 | 4.6 | 2.4 | 1 |